Dynamics of ion channeling at low energies: Preliminary trajectory studies

John E. Adams and Jimmie D. Doll

Citation: The Journal of Chemical Physics **73**, 2137 (1980); doi: 10.1063/1.440409
View online: http://dx.doi.org/10.1063/1.440409
View Table of Contents: http://scitation.aip.org/content/aip/journal/jcp/73/5?ver=pdfcov
Published by the AIP Publishing

Dynamics of ion channeling at low energies: Preliminary trajectory studies

John E. Adams and Jimmie D. Doll[a)]

University of California, Los Alamos Scientific Laboratory, [b)] *Los Alamos, New Mexico 87545*
(Received 7 April 1980; accepted 14 May 1980)

In order to understand better recent experiments which have examined the channeling of deuterium ions in tungsten single crystals at low incident energies, we have computed classical trajectories using various sets of ion–atom interaction parameters. Both the penetration depth profiles and the backscattered ion energy spectra display strong dependences upon the particular input parameters but to a much lesser extent upon the level of accuracy to which the individual trajectories are calculated. On the basis of our results we are able to suggest experiments which may resolve present uncertainties about the appropriate description of the microscopic interaction forces.

I. INTRODUCTION

When Robinson and Oen[1] predicted on the basis of computer simulations that ion bombardment of a crystal lattice should be characterized by anomalously long-range penetration of ions along the major crystallographic axes, it was recognized that the channeling effect provides a unique opportunity for the investigation of ion–solid interactions.[2] Most notably, the work of Lindhard,[3] which is founded on the replacement of sums of individual ion–atom potentials with a suitable continuum potential, has produced a model for the channeling of ions in the kilovolt to megavolt energy range which has met with so much success that subsequent studies have in general not found it necessary to improve on its fundamental dynamical description. Nevertheless, it is clear that there is a low-energy regime (<1 keV) within which the assumptions of Lindhard's theory are of questionable validity. This breakdown of the formulation at low ion velocities occurs as a result of the reduced correlation of the steering collisions with the atoms which define the channel boundary. Thus, one is forced to discard the continuum potential model at these energies, even though no one has been successful in constructing an analogous formalism which treats these potentially more erratic "slow" channeling trajectories.

It should be noted that interest in dynamics within the low-energy regime is not merely academic; several high-technology applications of channeling phenomena have made a better understanding of the ion dynamics increasingly necessary. For example, the problem of radiation damage to the inner walls of fusion reactors and the associated complication whereby ions are reflected from the walls back into the confined plasma constitute important considerations in the investigation of controlled thermonuclear reactions.[4] A second area in which there seems to be a developing interest is ion beam lithography,[5] a technique which may make possible structure fabrication below the half-micron lower limit of conventional photolithography. Then, too, one may expect that a bombardment in the energy region below a kilovolt will afford yet an additional degree of versatility in the already important field of ion implantation of semiconductor devices.[6]

It is on the basis of a recent experiment of Panitz,[7] however, that one of the potentially most useful applications of channeling may be the solution of problems in surface structure determination and, in particular, in the location of adsorbed species. In that experiment an 80 eV deuteron beam incident upon a tungsten single crystal was shown to yield a reproducible penetration depth distribution of the implanted ions which differs markedly from that which would be predicted by conventional theory.[3] Specifically, the results are seen to exhibit a definite structure, whereas the dynamical basis of the Lindhard work suggests that one should obtain only a fairly featureless bimodal distribution. In order to make some sense of these surprising observations, Brice[8] has constructed a simple, essentially geometrical theory which does indeed predict that if adsorbed impurity molecules are present on the surface, then at these low energies the spatial distribution of the ions which come to rest within the crystal should display a structure which roughly resembles that seen by Panitz, although a quantitative agreement between theory and experiment has not been demonstrated. Even so, one expects that, inasmuch as the surface geometry of the crystal constitutes the primary restriction on the direction of ions into particular axial and planar channels, the measured depth profile may be altered appreciably by a simple change in the orientation of the outermost atomic layer. One would thus have a sensitive probe of such effects as surface reconstruction and adsorbate binding, processes which are not always identifiable unambiguously via conventional LEED or atomic diffraction techniques.

As a first step in the analysis of ion dynamics in ordered solids, we report here the calculation of individual deuterium ion trajectories. These computed trajectories differ from those obtained by Robinson and co-workers[9] principally as a result of our implicit inclusion of dynamical effects which cannot be attributed to sequential, isolated, two-body collisions. It has been our experience that fairly long-range potential effects do have such a significant influence on the overall trajectory that the introduction of more realistic dynamics into our calculations seems imperative. In addition, we

---

[a)] A. P. Sloan Fellow.

[b)] Work supported by the U. S. Department of Energy.

 0021-9606/80/172137-08$01.00

have chosen initially to confine our studies to channeling within a rigid lattice where the atoms are fixed at their equilibrium positions. The expectation is that, even without the possibility of energy loss via phonon creation (the only energy loss mechanism included being loss to the electronic degrees of freedom), a great deal of information may be extracted from the results. Further assessments of the quality of our model and of our calculations are discussed in detail in later sections.

II. THEORY

One commonly proceeds in the description of the motion of an ion in the "field" of an ordered solid by dividing the net forces on the ion into two categories, namely, elastic and inelastic interactions.[10] The elastic contribution, (i.e., the contribution to the potential which conserves total energy) is essentially repulsive and depends only upon the relative position of the ion with respect to all the atoms of the lattice. On the other hand, the inelastic (or nonconservative) forces incorporate the available energy loss mechanisms and may depend, in general, on both the position and the velocity of the ion. Unfortunately, very little is known about the details of the forces on ions moving at these low velocities; however, it is reasonable to adopt, as a first guess, some of the same functional forms which find use in studies of channeling at higher energies.

A. Elastic potential

There is a general agreement among workers in this field that the most appropriate model for the conservative ion–atom interaction is some sort of screened Coulombic potential.[2] One of the most widely used functions (and the one which will be adopted herein) is an approximation by Moliere to the Thomas–Fermi potential[11]

$$V(r) = \frac{Z_1 Z_2 e^2}{r}\left(0.35\, e^{-(0.3)r/a_{TF}} + 0.55\, e^{-(1.2)r/a_{TF}} + 0.1\, e^{-6r/a_{TF}}\right), \tag{2.1}$$

where here Z_1 and Z_2 are, respectively, the atomic numbers of the ion and solid atom, e is the electron charge, r is the distance between the ion and a particular lattice atom, and a_{TF} is the Thomas–Fermi screening radius. For our purposes it is convenient to take a_{TF} to be given by a scaled version of the modification proposed by Firsov[12]:

$$a_{TF} = K_{el}\cdot\left(\frac{9\pi^2}{128}\right)^{1/3} a_B (Z_1^{1/2} + Z_2^{1/2})^{-2/3}, \tag{2.2}$$

with a_B being the Bohr radius and K_{el} representing an adjustable scaling constant (in Firsov's result $K_{el}=1$).[13] It may be easily seen that an increase (a decrease) in the value of K_{el} corresponds to a narrowing (widening) of the channels.

One may now proceed to a determination of the total potential by summing over the contributions from all the atoms which lie within some critical distance r_c from the ion, with r_c being enlarged until further expansion results in no change in V. However, in order that one may obtain a converged sum using individual two-body potentials given by Eq. (2.1), it appears necessary to compute interactions with a large number of solid atoms, the result being that the calculation consumes a large amount of computer time. We were thus led to the investigation of another method for performing the direct summation over neighboring lattice sites which seemed to hold the promise of allowing us to generate more accurate trajectories and simultaneously to reduce the actual run time. The formalism for such a method has been described by Steele[14] and consists of a Fourier analysis of the potential contribution from a plane of atoms parallel to the surface. For the present case in which the potential function is just the sum of Yukawa potentials, Steele's analysis is particularly simple. The details of the application of this model are given in the Appendix. It should be further noted that, inasmuch as the Fourier analysis is performed for a particular atomic plane (rather than for the crystal as a whole), it becomes a very simple matter to construct hybrid potential summations which consist of both direct summations over certain planes and a summation via Steele's method over the remaining layers. In practice, it appears that such a hybrid technique is of the most practical utility (see Sec. III for the details of the calculations).

B. Inelastic force

As indicated in the Introduction, the only nonconservative force included in this study is the one which accounts for the loss of energy via electronic excitations of the solid. Such excitations may be viewed classically in terms of an equivalent frictional force which acts upon the ion while it is within the crystal. Essentially, the sea of electrons in the solid exerts a "viscous drag" on the moving particle just as if the electrons actually constitute a fluid through which the ion passes. From this picture one would conclude that this friction should be directly proportional to the ion velocity, a view which is borne out by more detailed considerations of a particle moving through an electron gas.[15] It is known empirically that the macroscopic energy loss of an ion having a particular translational energy is well described by an expression of the form[16]

$$-\frac{dE}{dz} = K_{inel} E^{p}, \tag{2.3}$$

where K_{inel} is an appropriate scaling parameter and p is a number whose magnitude is dependent upon the particular energy regime being studied (and thus upon the dynamics of the ion at those energies). At low energies one finds that $p=\frac{1}{2}$ gives a satisfactory description of the stopping behavior. (This behavior is essentially that which was predicted by Fermi and Teller[15] for particle velocities much less than the Fermi velocity of the electrons of the solid.)

Of course, one must realize that Eq. (2.3) is strictly applicable only to the description of the macroscopic energy loss. It is not at all clear how one goes about modeling the microscopic loss mechanism, i.e., the true frictional force felt by the ion at any particular point of a trajectory. For example, it seems reasonable to expect that the energy loss should depend not only upon the ion's velocity but also upon its position within

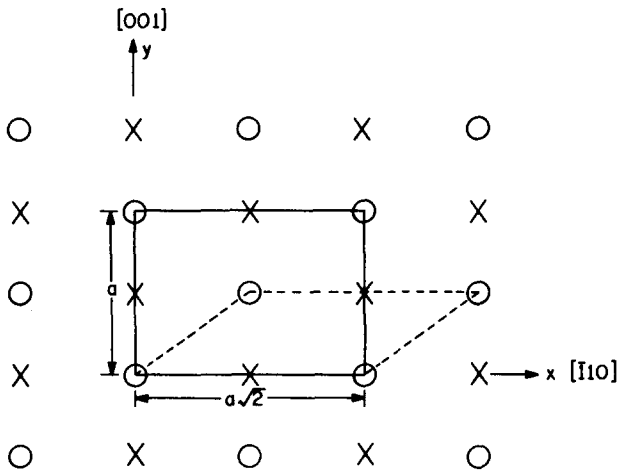

FIG. 1. The W(110) surface, showing both the rectangular lattice cell (solid lines) and the primitive lattice cell (broken lines). The positions of atoms in the outermost layer are indicated by the open circles (o), while the projection of the atoms of the second layer is denoted by crosses (×).

the crystal since in fact the electrons of the solid do not represent a perfectly uniform charge density. However, even with this important caveat, we have chosen to take Eq. (2.3) as a model for the microscopic inelasticity contribution partly as a result of its particular simplicity and partly because no obvious replacement candidate exists.

At this juncture it is perhaps appropriate to comment further upon our decision to ignore the inelastic contribution from the heavy-particle degrees of freedom. We certainly acknowledge the fact that phonon excitation is likely to represent a very significant mechanism by which the ion's energy is dissipated. One must remember, though, that such a process requires that the ion undergo a close collision with one of the solid atoms. Clearly, any well-channeled ions must, by virtue of the fact that they are directed more or less down the center of the channels and away from the atomic boundary planes, participate in very few of these encounters. The result is then that long-range penetration is accompanied by few phonons being created, and hence electronic stopping must constitute the primary inelastic event for these ions whose trajectories are of most interest to us. Those particles which *do* lose most of their energy while undergoing a large number of close collisions constitute an essentially "randomly" scattered fraction which one might expect to be described fairly well by the conventional analysis given by Lindhard[3] for such ions, i.e., that they would appear in the depth profile as a featureless, wide peak lying within the first few solid layers. Admittedly, our formulation will not describe well this component of the profile (for instance, we are likely to see an increased number of particles which, because they do not lose energy rapidly enough, escape from the solid after penetrating a few layers); however, since very little information seems to be obtainable from this random fraction, we have concluded that the static lattice model may not be too restrictive, at least as a first approximation. Experimentally, one would expect that dechanneling as a result of displacements of the atoms which define the channel boundaries will increase the observed background at intermediate depths (as predicted by Lindhard[3]) but will probably not significantly alter any structure seen in the depth profile.

III. RESULTS

Classical trajectories were computed for 80 eV deuterons impinging upon a clean (110) tungsten crystal face. A typical run consisted of 441 trajectories, each beginning well above the surface ($z_0 \approx 15$ a.u.) with momentum normal to the surface plane. The initial x and y coordinates were chosen from a rectangular grid of points distributed over the centered surface lattice cell shown in Fig. 1 via the rule

$$(x_0, y_0) = \left(n \frac{a\sqrt{2}}{20}, \; m \frac{a}{20}\right), \qquad (3.1)$$

$$n, m \in \{0, 1, 2, \cdots, 20\}$$

(a is the cubic bcc lattice dimension). As indicated in the previous section, there are two parameters K_{el} and K_{inel} which must be specified in order that the motion be determined. We have not attempted in this study to extract the "best" set of parameters, but rather have centered our attention on an examination of the effect which a change in either or both of those parameters has on two different types of results, the ion penetration depth distribution, and the energy spectrum of the ions backscattered by the crystal. In Sec. IV we suggest, however, appropriate experiments which could lead to an accurate determination of these two quantities.

Our choices for K_{el} were made from the range of values suggested by workers interested in surface reflection effects such as semichanneling.[17–19] That range extends from about 0.6 to 1.0 and is sufficiently wide that one would expect a radical change in the ion dynamics as one proceeds from one end of the interval to the other. Having no reason for choosing initially one particular value, we generated a few sample trajectories in order to get a feel for how the channel widths depend on the value of K_{el}. Those test runs indicate an appropriate scaling constant to be about 0.7, since for this value the resulting channel widths seem of the right magnitude to yield the kind of behavior seen by Panitz.[7] However, inasmuch as it is desirable to have a better picture of the overall dependence of the dynamics on K_{el}, we have also generated a full set of trajectories for $K_{el} = 0.85$.

Prior to discussing the results calculated for these two choices for K_{el}, we should describe our method for determining the inelastic scaling parameter K_{inel}. An estimate of the proper value may be taken from Brice's work,[8] wherein he suggests that $K_{inel} = 0.179\,(\text{eV})^{1/2}/\text{Å}$ appropriately scales the energy loss in the [110] axial channel, with K_{inel} being larger for the various planar channels. (The Fermi–Teller[15] energy loss formula would predict a value of K_{inel} only about a third as large as that suggested by Brice.) However, of course, it is not necessarily true that Brice's value will produce the best answer in the present work because Eq. (2.3) is

being used to model the microscopic rather than the macroscopic energy loss. Thus, we have chosen to scale the inelastic force by adjusting the magnitude of K_{inel} (given a choice for K_{el}) until the ions having the maximum penetration come to rest within roughly 50 layers, which is the farthest extent of the channeling seen by Panitz.[7] Presumably, these special trajectories are those with $(x_0, y_0) = (a\sqrt{2}/4, a/4)$, $(3a\sqrt{2}/4, a/4)$, $(a\sqrt{2}/4, 3a/4)$, and $(3a\sqrt{2}/4, 3a/4)$, since they represent ions impinging along the [110] channel axis. The possible difficulty with this method is that these perfectly channeled trajectories may actually be absent in the experiments, and instead may correspond to ions which have traveled so far into the crystal and have become sufficiently separated from the bulk of the stopped particles that they are not detected. Alternatively, if surface impurities should be located so as to block the open channel, then no perfect channeling would be possible. If such problems should indeed be important, then the scaling must be determined instead either by matching particular profile structure with the existing experimental results or by performing independent experiments which would fix the value. In the absence of such information, however, we have used the *ad hoc* method described above to estimate a value for K_{inel} of 0.135 $(\text{eV})^{1/2}/\text{Å}$ when K_{el} is taken to be 0.7.

The trajectories themselves were constructed by the integration of Hamilton's equations using a fifth-order, variable step Adams–Moulton predictor–corrector algorithm.[20] Numerous test runs have shown that the depth to which an ion with a particular set of initial coordinates penetrates depends quite strongly upon the value adopted for the integrator error limit ϵ. Other results have indicated that the range over which direct summations of the elastic potential are performed can also drastically alter a trajectory even though the long-range potential contributions represent only a small fraction of the total. Yet it is not quite so obvious that the gross structure of the depth distribution will exhibit this same sensitivity to the "quality" of the calculations as do the individual trajectories. We therefore have, for particular K_{el} and K_{inel}, run two complete sets of trajectories which differ only with respect to the amount of work put into constructing them. The comparison here should allow us to evaluate the feasibility of carrying out large numbers of these computations under a variety of initial conditions.

A. Dependence on potential energy summation

In Fig. 2 we give two calculated depth distributions obtained using $K_{\text{el}} = 0.7$ and $K_{\text{inel}} = 0.135$ $(\text{eV})^{1/2}/\text{Å}$. Histogram (a) is derived from trajectories which were computed with an integrator error limit[20] of 10^{-6} via a truncated direct summation of the elastic potential. Specifically, the included interactions extended over 28 lattice atoms per layer and as many as five (110) layers. In contrast, the potential summation used in the calculation of histogram (b) represents a hybrid method, whereby interactions with atomic layers lying within 4 a.u. of the ion were summed directly while the contribution coming from the remaining layers was obtained from the first few terms of a Fourier analysis. (A maximum of nine layers were included in the calculation, with the direct summation involving 128 two-body interactions per layer. These trajectories were computed using an error limit equal to 10^{-7}.) We found this hybrid technique to be advantageous for two reasons: First, such an extensive summation performed only by direct means requires a prohibitively large amount of computer time, and second, Steele's Fourier analysis method[14] fails in practice when the ion is near an atomic plane (a few periodic functions do a poor job of mirroring the short-range repulsive forces).

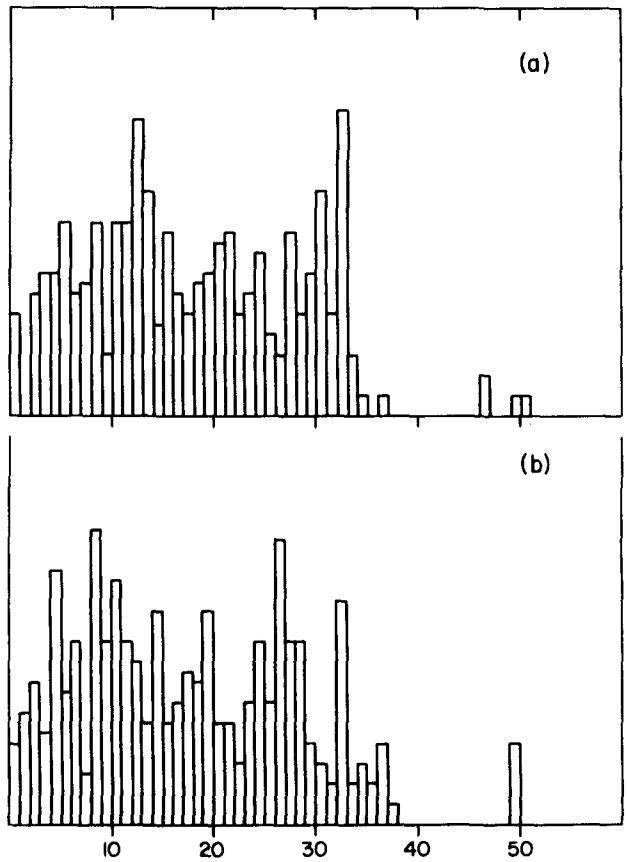

FIG. 2. The penetration depth distributions [$K_{\text{el}} = 0.7$ and $K_{\text{inel}} = 0.135$ $(\text{eV})^{1/2}/\text{Å}$] obtained using (a) a truncated direct summation and (b) the hybrid summation described in the text. The width of the boxes corresponds to one interlayer spacing (≈ 2.23 Å).

The most obvious similarity between the two calculations is that each yields essentially the same envelope of ion ranges. For example, although the profiles appear to be continuous within the depth range extending from the surface to about the 35th layer, one observes a broad gap in both distributions beyond that range, with only the few "best-channeled" trajectories appearing at about the 50th layer. This gap structure may indicate that the difficulty anticipated above concerning the determination of the inelastic scaling parameter, i.e., that the most deeply penetrating ions are not detected in the experiment, does indeed warrant consideration.

One would like, though, to make a more quantitative comparison between the two sets of results. To this

TABLE I. Analysis of depth distributions.

K_{el}	K_{inel}	$\langle z \rangle$[a]	$\sigma (= \sqrt{\langle z^2 \rangle - \langle z \rangle^2})$
0.70	0.135 (Calc. I)[b]	18.1	10.6
0.70	0.135 (Calc. II)[c]	18.6	10.2
0.70	0.110	21.2	11.8
0.85	0.135	10.4	6.95

[a]Mean penetration depth given in units of the (110) interlayer spacing (2.23 Å).
[b]Calculation done using the hybrid potential summation described in Sec. III.
[c]Calculation done using the truncated direct summation of the potential described in Sec. III.

end we have calculated the first few moments of the distributions and have summarized our findings in Table I. It is immediately clear that, even though the structural details of the pair of depth distributions do vary somewhat, the values calculated for the mean penetration depth $\langle z \rangle$ and the standard deviation σ differ by only 3%–4%. Thus, one finds that the overall depth profile is fairly insensitive to the method by which the elastic potential contributions are obtained. Such behavior, however, does not extend to individual ion trajectories. An example of the much stronger dependence on the elastic potential exhibited by a particular trajectory is depicted in Fig. 3. Here we have plotted the z component of the ion's position versus the time. Notice that although initially either summation method seems to generate accurately the correct path, as time progresses small errors in the truncated direct sum are compounded to the point that the trajectories diverge radically. In a system of many scattering centers such as this, it is to be expected that seemingly minor computational errors can quickly destroy the accuracy of a particular trajectory.

An additional comparison of the results obtained with differing potential summations can be made by examining the energies of the ions which are backscattered by the crystal. Such an energy analysis is shown in Fig. 4. Note that the two histograms are essentially identical

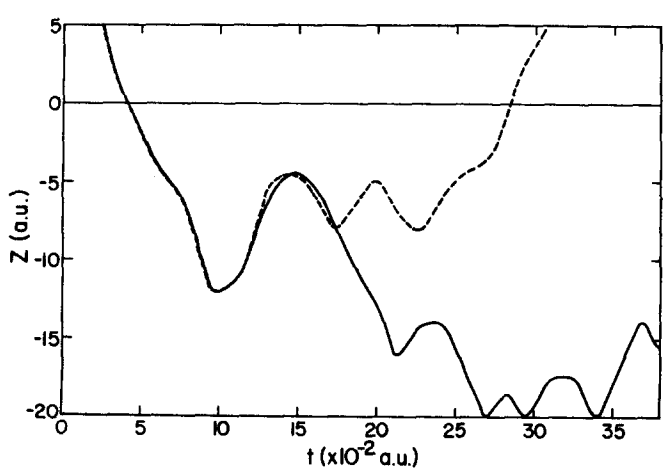

FIG. 3. The time evolution of the z coordinate of the $(x_0, y_0) = (\sqrt{2}a, 0.85a)$ trajectory as computed via a truncated direct summation (broken line) and a hybrid potential summation (solid line).

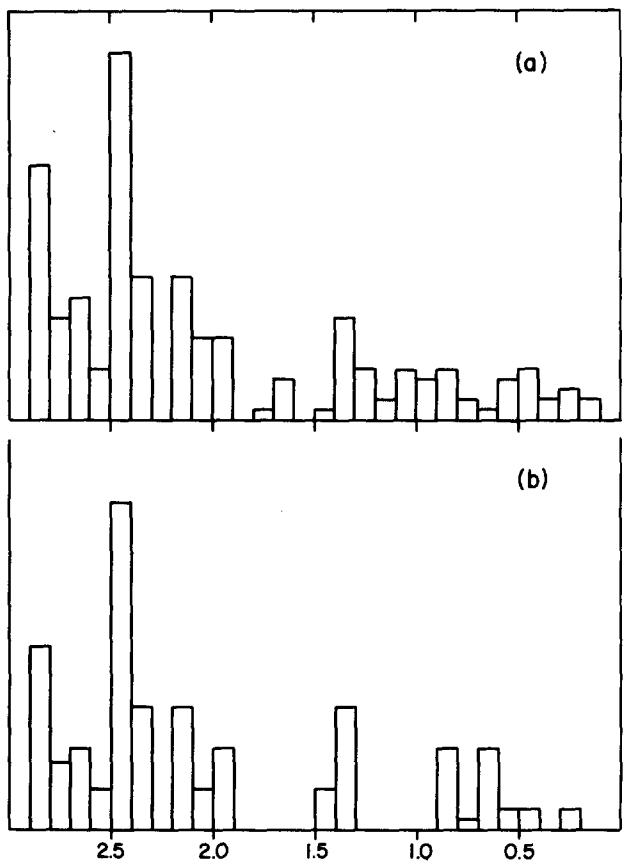

FIG. 4. Energy analysis of the backscattered ions [(a) and (b) here are the same as in Fig. 2]. The energy boxes are 0.1 a.u. ($\approx$ 2.72 eV) in width.

down to a final ion energy of 1.8 a.u. ($\approx$ 50 eV); any comparisons at lower energies, i.e., at greater energy losses, are not really significant inasmuch as such results are derived from ions "randomly" scattered within the solid and are thus not expected to be accurate in the rigid lattice approximation. The two major peaks appearing at $E > 2.4$ a.u. are of particular interest since they correspond, roughly, to a direct reflection from the first or second solid layer, thus implying that their relative separation should be particularly sensitive to the value of the inelastic scaling parameter used in the calculations. Fortunately, it appears that even a truncated summation will be sufficient in order to fix that separation.

B. Dependence on scaling parameters

The calculations done for various values of K_{el} and K_{inel} were performed using the truncated direct summation technique described above. Again we have generated the depth profiles and backscattered ion energy analyses, with the results being displayed in Figs. 5 and 6, respectively. In each case one finds the dependence of the observed behavior upon the scaling parameters to be quite dramatic, although not unexpected. For example, an increase in K_{el} from 0.7 to 0.85 should represent physically a constriction of the channels, this width reduction being reflected in an increase in the hard sphere scattering radius for the ion–atom collision. Consequently, long-range channeling should become in-

creasingly difficult and the mean penetration depth should be reduced. Likewise, the increased frictional force arising from an increase in K_{inel} from 0.110 to 0.135 $(eV)^{1/2}/Å$ should be manifested in a general shift of the depth distribution toward the surface. Both of these anticipated effects are indeed reproduced in our calculations.

Here, too, one finds it useful to quantify the relationship between the scaling parameters and the overall distributions. The calculated mean penetration depths and standard deviations given in Table I show the trends indicated above quite clearly. Notice that the value of $\langle z \rangle$ is reduced by about 40% by a 20% increase in K_{el}, whereas roughly the same sort of change in K_{inel} results in only a 14% increase in the mean penetration. Clearly, it is the value adopted for the elastic scaling parameter which will be reflected most sensitively in the first moment of the distribution. Since the same sort of dependence can be seen in the computed standard deviations, we conclude that if depth profiles are of primary interest, then the most effort should be put into an accurate determination of K_{el}, with the adjustment of K_{inel} essentially representing only "fine tuning."

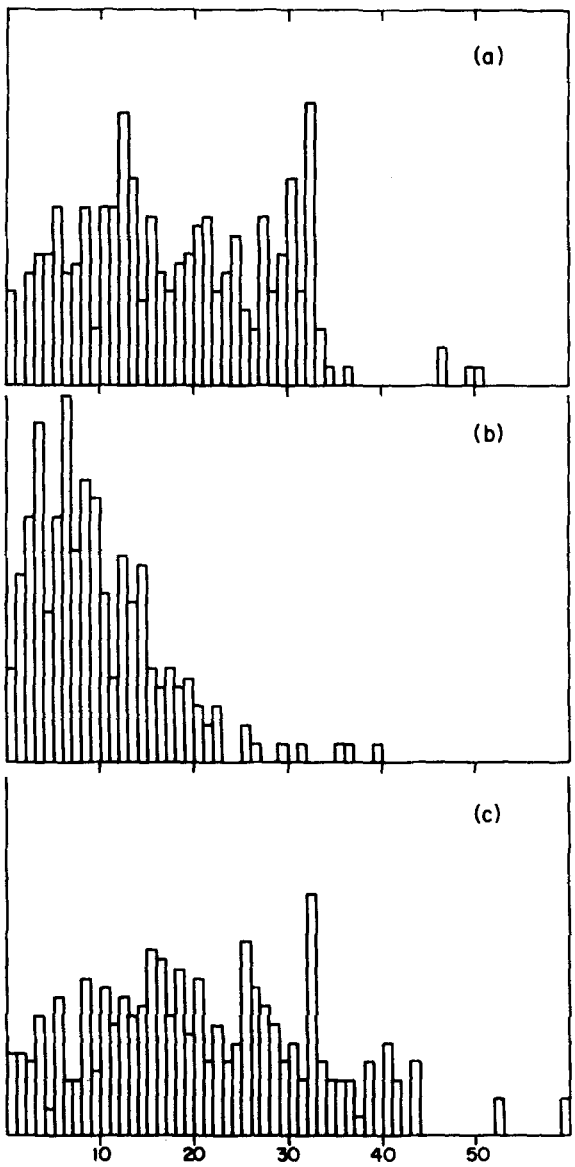

FIG. 5. Penetration depth distributions for (a) $K_{el} = 0.7$ and $K_{inel} = 0.135$ $(eV)^{1/2}/Å$, (b) $K_{el} = 0.85$ and $K_{inel} = 0.135$ $(eV)^{1/2}/Å$, and (c) $K_{el} = 0.7$ and $K_{inel} = 0.110$ $(eV)^{1/2}/Å$.

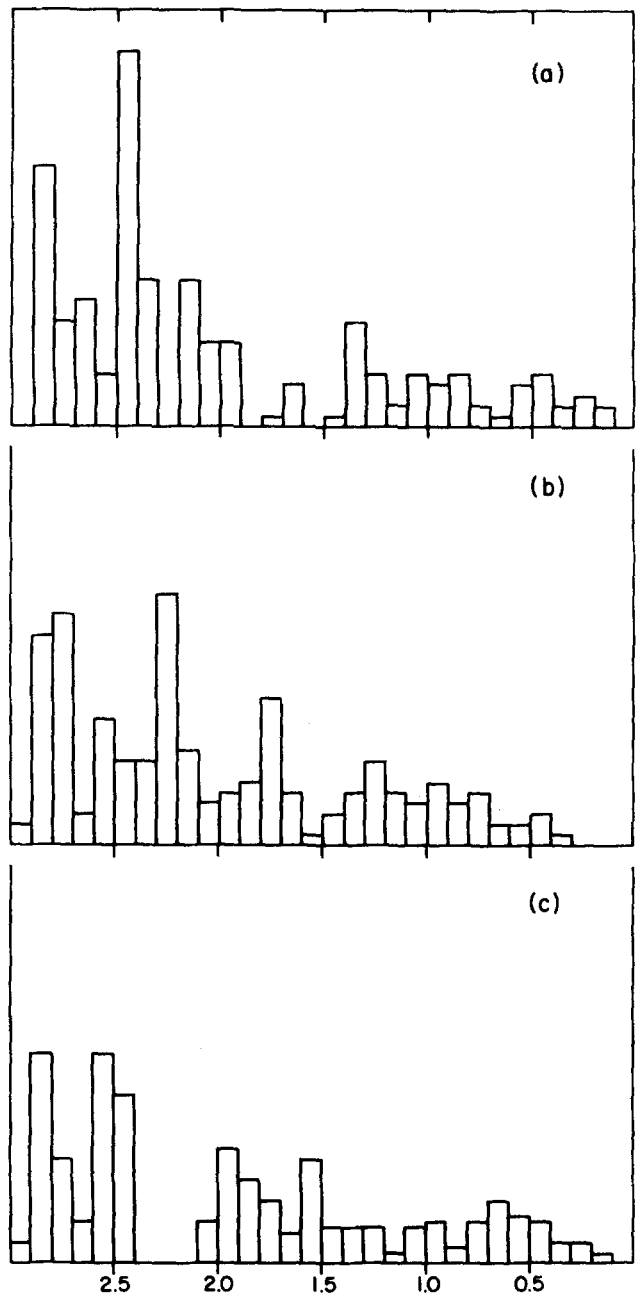

FIG. 6. Backscattered ion energy analysis for the sets of trajectories shown in Fig. 5.

Fortunately, the backscattered ion energy analysis affords us the opportunity to fix this inelastic scaling to which the mean penetration is relatively insensitive. Here we make use of the observation (seen in Fig. 6) that the separation between the two principal high-energy peaks exhibits a direct dependence upon K_{inel}. This separation can be seen to decrease in the two histograms obtained with $K_{el} = 0.7$ when the inelastic scaling is decreased. However, one should also note that the situa-

tion may be complicated by the fact that an alteration of K_{el} also leads to an effective change in the friction. (This effect may be seen in the increase in the peak separation which accompanies an increase in K_{el} from 0.7 to 0.85 while K_{inel} is held fixed. Inasmuch as a larger K_{el} essentially represents an increased background potential energy and hence a diminished ion kinetic energy, the velocity-dependent friction force on the average will be reduced.) Such an energy analysis should nonetheless permit one to estimate K_{inel} when used in conjunction with a definitive method for determining the elastic scaling.

IV. DISCUSSION

The principal conclusion to be drawn from this work is that, inasmuch as within the low-energy collision regime the motion of channeled ions depends very strongly upon the parameterization of the ion–solid interaction, it appears reasonable to expect that one could extract considerable detailed information about the forces which determine the dynamics of a given scattering system. Consequently, it should indeed be possible to detect experimentally the presence of adsorbates or, more generally, of surface layers which are of a different registry from that of the bulk. (Calculations which explore this important application of ion channeling are currently in progress.) On the other hand, our trajectories have shown that, since certain gross features of the ion scattering may be generated with relatively little effort, computer simulations can be particularly useful in sorting out the influences of various assumed interactions on the channeling dynamics.

In the absence of reliable experimental information about the details of the ion–solid forces, one might think that analytical applications of channeling phenomena would be merely qualitative in nature. The present work, however, has suggested experiments which should accurately yield the appropriate scaling parameters appearing in the classical equations of motion. For example, the elastic potential scaling constant K_{el} has been shown to influence critically the mean penetration depth of the injected ions. Measurements of that depth when compared with suitable calculations should therefore lead to much improved estimates of the range of the conservative forces. However, then, too, one can get a value for the inelastic scaling parameter K_{inel} by analyzing the energy spectrum of the ions backscattered from the crystal. We indicated in Sec. III that the relative positions of the two strong high-energy peaks in this spectrum are, for a given K_{el}, determined by the friction scaling. Since such peak measurements need to be made over only a small energy range, it is hoped that they may be performed with little difficulty. (One should also note that the trajectory studies appear to be able to reproduce these peaks very accurately for given interaction parameters. In addition, relaxation of the rigid lattice approximation used in this paper so as to allow heavy-particle energy losses will lead only to a broadening of these particular spectral details and will not affect their relative separation. Indeed, none of the fundamental structure appearing in the depth distributions should be destroyed by the introduction of lattice atom motion, although surely one would expect to see additional peak broadening and an increase in the dechanneled background.)

Overall one sees in these calculations just how sensitively channeling dynamics depends upon the relatively long-range component of the ion–atom potential. Such a dependence brings into question the practice of truncating such interactions so as to consider only isolated two-body collisions, although apparently these limited range summation methods do permit one to obtain most of the gross structure of the channeling results. Furthermore, one sees that continuum potential models will be inapplicable in the low-energy regime since in general the trajectories are more erratic than their more energetic counterparts. Thus, one is drawn naturally to the more detailed study of channeling dynamics, the first investigations of which are given here. Further studies will center on more quantitative evaluations of the effects of such things as the presence of overlayers and the thermal motion of the solid lattice.

APPENDIX

Steele[14] writes the total elastic potential as

$$V(\mathbf{r}) = \sum_{\mathbf{g}} \sum_{\alpha} w_{\mathbf{g}}(z_\alpha)\, e^{i\mathbf{g}\cdot\boldsymbol{\tau}} , \tag{A1}$$

where $\mathbf{r}$ is the position vector of the ion, $\boldsymbol{\tau}$ is the projection of $\mathbf{r}$ onto a unit cell, $\mathbf{g}$ is defined to be a multiple of the reciprocal lattice vectors $\mathbf{b}_1$ and $\mathbf{b}_2$ as

$$\mathbf{g} = 2\pi[g_1\mathbf{b}_1 + g_2\mathbf{b}_2] , \quad g_1, g_2 \in \{0, \pm 1, \pm 2, \ldots\} ,$$

and $w_{\mathbf{g}}(z_\alpha)$ is the Fourier component (a function of z_α, the distance from the ion to the αth plane). Without reproducing Steele's development, we indicate here only the general result for the Fourier components

$$w_{\mathbf{g}}(z_\alpha) = \frac{2\pi}{a_s} \sum_{k} e^{i\mathbf{g}\cdot\mathbf{m}_k} \int_0^\infty dt\, t J_0(gt)\, e_{gs}(\rho) , \tag{A2}$$

with a_s being the area of a surface lattice cell, $\mathbf{m}_k$ being the position vector of the kth atom in the unit cell, $\mathbf{t} = \boldsymbol{\tau} + \mathbf{l} + \mathbf{m}_k$ ($\mathbf{l}$ being defined as the location of a particular unit cell), and $e_{gs}(\rho)$ being the interaction of the ion with the lattice atom located at a distance ρ, i.e., $\rho = (z_\alpha^2 + t^2)^{1/2}$.

For a potential of the Yukawa type

$$e_{gs}(\rho) = \beta \frac{e^{-\gamma\rho}}{\rho} , \tag{A3}$$

substitution into Eq. (A2) and subsequent integration over t yields

$$w_{\mathbf{g}}(z_\alpha) = \frac{2\pi}{a_s} \beta \frac{e^{-z_\alpha\sqrt{\gamma^2+g^2}}}{\sqrt{\gamma^2+g^2}} \sum_{k} e^{i\mathbf{g}\cdot\mathbf{m}_k}$$

$$= \frac{2\pi}{a_s} \beta \frac{e^{-z_\alpha\sqrt{\gamma^2+g^2}}}{\sqrt{\gamma^2+g^2}}$$

for the rhombic (110) unit cell of tungsten. Thus, one finds that now Eq. (A1) has become

$$V(\mathbf{r}) = \frac{2\pi}{a_s} \beta \sum_{\alpha} \sum_{\mathbf{g}} \frac{e^{-z_\alpha\sqrt{\gamma^2+g^2}}}{\sqrt{\gamma^2+g^2}} e^{i\mathbf{g}\cdot\boldsymbol{\tau}} . \tag{A4}$$

Since coordinates may be chosen such that $w_{\mathbf{g}} = w_{-\mathbf{g}}$, Eq. (A4) may be rewritten as a real cosine series, namely,

$$V(\mathbf{r}) = \frac{2\pi}{a_s}\,\beta \sum_{\alpha}\left[\frac{e^{-\varepsilon_\alpha \gamma}}{\gamma} + 2\sum_{\mathbf{g}'} \cos(\mathbf{g}'\cdot\boldsymbol{\tau})\,\frac{e^{-\varepsilon_\alpha\sqrt{\gamma^2+g'^2}}}{\sqrt{\gamma^2+g'^2}}\right],$$

where now $\mathbf{g}'$ represents only the "positive" g vectors (e.g., $g_1 > 0$, $|g_2| \geq 0$). It is also convenient for trajectroy calculations to transform the τ vectors, originally given in terms of the lattice vectors, into their Cartesian analogs. If one performs this transformation, one obtains the following result in terms of the x and y coordinates of the ion:

$$V(\mathbf{r}) = \frac{2\pi}{a_s}\,\beta \sum_{\alpha}\left[\frac{e^{-\varepsilon_\alpha \gamma}}{\gamma} + 2\sum_{\mathbf{g}'} \frac{e^{-\varepsilon_\alpha\sqrt{\gamma^2+g'^2}}}{\sqrt{\gamma^2+g'^2}}\cos(G_x x + G_y y)\right],$$

$$G_x \equiv \frac{2\pi g_1}{a\sqrt{2}}\,, \tag{A5}$$

$$G_y \equiv \frac{2\pi}{a}\,(2g_2 - g_1)$$

(a is just the cubic lattice dimension for the tungsten bcc crystal).

Equation (A5) thus makes calculation of $V(\mathbf{r})$ and its Cartesian derivatives simple for the potential function given in Eq. (2.1).

[1] M. T. Robinson and O. S. Oen, Appl. Phys. Lett. 2, 30 (1963); Phys. Rev. 132, 2385 (1963).

[2] There are several good reviews of work on channeling phenomena. Two of the best are S. Datz, C. Erginsoy, G. Leibfried, and H. O. Lutz, Annu. Rev. Nucl. Sci. 17, 129 (1967); and D. V. Morgan, *Channeling* (Wiley, London, 1973).

[3] J. Lindhard, K. Dan. Vidensk. Selsk. Mat.-Fys. Medd. **34** (14), 1 (1965).

[4] J. T. Hogan and J. F. Clarke, J. Nucl. Mater. 53, 1 (1974).

[5] E. D. Wolf, Phys. Today 32, 34 (1979).

[6] See, for example, G. Carter and W. A. Grant, *Ion Implantation of Semiconductors* (Wiley, New York, 1976).

[7] J. A. Panitz, J. Vac. Sci. Technol. 14, 502 (1977).

[8] D. K. Brice, Phys. Rev. B 18, 990 (1978).

[9] M. T. Robinson and I. M. Torrens, Phys. Rev. B 9, 5008 (1974); O. S. Oen and M. T. Robinson, Nucl. Instrum. Methods 132, 647 (1976); Am. Inst. Phys. Conf. Ser. 28, 329 (1976).

[10] N. Bohr, K. Dan. Vidensk. Selsk. Mat.-Fys. Medd. 18 (8), 1 (1948).

[11] G. Moliere, Z. Naturforsch. Teil A 2, 133 (1947).

[12] O. B. Firsov, Sov. Phys. JETP 6, 534 (1958).

[13] See, for example, D. J. O'Connor and R. J. MacDonald, Radiat. Eff. 34, 247 (1977).

[14] W. A. Steele, Surf. Sci. 36, 317 (1973); 39, 149 (1973). Very similar work has been performed by N. Cabrera and F. O. Goodman, J. Chem. Phys. 56, 4899 (1972), although those workers summed explicitly over the crystal layers. For our purposes it is more convenient to know the contribution from each layer separately.

[15] E. Fermi and E. Teller, Phys. Rev. 72, 399 (1947).

[16] M. T. Robinson, in *Interatomic Potentials and Simulation of Lattice Defects*, edited by P. C. Gehler, J. R. Beeler, Jr., and R. I. Jaffe (Plenum, New York, 1972), p. 281.

[17] D. S. Karpuzov, D. G. Armour, and I. N. Evdoimov, Radiat. Eff. 41, 141 (1979).

[18] B. Poelsema and A. L. Boers, Radiat. Eff. 41, 229 (1979).

[19] Y. Yamamura and W. Takeuchi, Radiat. Eff. 42, 55 (1979).

[20] W. H. Miller and T. F. George, J. Chem. Phys. 56, 5668 (1972).